Linewidth roughness and cross-sectional measurements of sub-50 nm structures with CD-SAXS and CD-SEM*

Chengqing Wang[a], Kwang-Woo Choi[b] Ronald L. Jones[a], , Christopher Soles[a], Eric K. Lin[a], Wen-li Wu[a†], James S. Clarke[c], John S. Villarrubia[d], Benjamin Bunday[e]

[a]Polymers Division, National Institute of Standards and Technology, Gaithersburg, MD, 20899-8541
[b]Intel Corporation, Santa Clara, CA
[c]Intel Corporation, Hillsboro, OR
[d]Precision Engineering Division, National Institute of Standards and Technology, Gaithersburg, MD
[e]International SEMATECH Manufacturing Initiative (ISMI), Austin, TX

ABSTRACT

Critical dimension small angle X-ray scattering (CD-SAXS) is a measurement platform that is capable of measuring the average cross section and sidewall roughness in patterns ranging from (10 to 500) nm in pitch with sub-nm precision. These capabilities are obtained by measuring and modeling the scattering intensities of a collimated X-ray beam with sub-nanometer wavelength from a periodic pattern, such as those found in optical scatterometry targets. In this work, we evaluated the capability a synchrotron-based CD-SAXS measurements to characterize linewidth roughness (LWR) by measuring periodic line/space patterns fabricated with extreme ultraviolet (EUV) lithography with sub-50 nm linewidths and designed with programmed roughness amplitude and frequency. For these patterns, CD-SAXS can provide high precision data on cross-section dimensions, including sidewall angle, line height, line width, and pitch, as well as the LWR amplitude. We also discuss the status of ongoing efforts to compare quantitatively the CD-SAXS data with top-down critical dimension scanning electron microscopy (CD-SEM) measurements.

Keywords: line width roughness, line edge roughness, small angle X-ray scattering, CD-SAXS

1. INTRODUCTION

The semiconductor industry has set a target for sub-nanometer amplitudes of line edge roughness (LER) and linewidth roughness (LWR) for extreme ultraviolet (EUV) lithography. The small scales of these features combined with the electron beam sensitivity of many photoresists challenge dimensional metrology based on electron and optical beam methods. Critical dimension small angle X-ray scattering (CD-SAXS) is a technique that may have the capability to quantify CD, pitch, line edge roughness and cross-sectional profile in periodic line and space (i.e., grating) structures.[1-6] The technique is based on transmission small angle X-ray scattering and uses a high energy X-ray beam to pass non-destructively through silicon substrates. As the beam passes through a periodic pattern, the diffracted intensity is recorded on a detector (Fig. 1). The CD-SAXS data are compared to data from measurements of linewidth, pitch, sidewall angle, and amplitude of LWR obtained from CD-SEM.

To systematically evaluate the capability of CD-SAXS for dimensional metrology, we designed a series of samples that provide a programmed, periodic line width roughness created by the placement of "tabs" of predetermined amplitude, size, and placement along the line edge. In our previous work, the samples were made of EUV photoresist; however, problems with ill-defined sidewall structures made comparing data quantitatively difficult.[7] To circumvent this difficulty, an EUV hardmask pattern was chosen for the present cross calibration effort. The resulting periodic roughness can be directly measured by a secondary, or "satellite,," diffraction axis where the intensities are directly

† Corresponding Author: wenli.wu@nist.gov

Metrology, Inspection, and Process Control for Microlithography XXII, edited by John A. Allgair, Christopher J. Raymond
Proc. of SPIE Vol. 6922, 69221Z, (2008) · 0277-786X/08/$18 · doi: 10.1117/12.773558

related to LER and LWR amplitude.[6] Results of these measurements can be used to assess the potential of the Debye-Waller method to measure LER in line/space patterned areas using CD-SAXS.

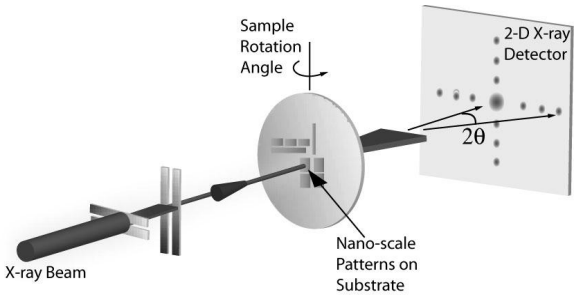

Fig. 1. Schematic of the CD-SAXS geometry, showing the measurements performed in transmission through a silicon substrate. The schematic illustrates the test patterns on the source side of the substrate; however, measurements with the patterns on the detector side of the substrate produce equivalent results. The experiments described here were performed with the patterns on the detector side of the substrate to reduce potential effects from beam damage. The beam is shown relative to the sample and the detector, illustrating the scattering angle, 2θ.

2. EXPERIMENTAL

A reticle with line/space patterns of programmed LWR was designed and fabricated for exposure using EUV lithography. The designed features include line/space arrays in patterned areas over an area exceeding 100 μm × 100 μm. Linewidth and line edge roughness samples with programmed roughness were created by adding "tabs,," similar to optical assist features common in photoresist image design, with a pre-determined distance between centers along the line edge, given the label "roughness wavelength." The distance of the tab edge from the nominal line edge is hereby referred to as the tab amplitude and ranges from 9 nm to 30 nm with a nominal roughness wavelength of 100 nm. Nitride with 60 nm thickness was patterned with 200 μm × 600 μm line/space gratings using EUV photolithography (λ = 13.6 nm). For this study, we have selected a LWR structure with a designed 35 nm linewidth, 250 nm pitch, and 15 nm programmed roughness amplitude to be printed on a 300 mm diameter wafer. The wafer was exposed by EUV with an 11 x 11 focus exposure matrix (FEM). The resulting nitride lines, which represent a hardmask that would result from an EUV lithography process, were consistent in demonstrating a trapezoidal profile and uniform profile height (i.e., did not exhibit height loss).

Thirty-six line measurements were performed per grating using CD-SEM in the Advanced Technology Development Facility (ATDF). In Fig. 2 (left), a representative CD-SEM image shows the periodic linewidth roughness in top-down view. This was achieved with an automated recipe that stepped a 3 x 3 matrix of regular (20 μm) intervals over the grating in both x and y directions, performing non-unique pattern recognition at each of the nine positions and placing a 2 μm long measurement image over four random lines at each position. CD and LWR values were calculated by the tool for all four lines in the image. Each image consisted of 512 line scans, allowing LWR to be calculated by the International SEMATECH Manufacturing Initiative (ISMI) best known method, which has been defined elsewhere.[7] This measurement scheme was also compatible with the new SEMI standard for LER measurement.[11] With this 36-line sampling plan, the error in estimating the mean CD and LWR by CD-SEM , is ≈ (0.1 to 0.2) nm.

CD-SAXS measurements were performed at the 5-ID-D beamline, operated by DND-CAT, at the Advanced Photon Source, part of Argonne National Laboratory, as described elsewhere.[4] As illustrated schematically in Fig. 1, CD-SAXS records the diffracted intensity from an array of patterns in transmission through a silicon substrate. An X-ray energy of E = 17 keV was selected using a monochromator, corresponding to a wavelength of λ = (0.0729 ± 0.0001) nm.[13] A focusing mirror and beam defining slits produced an approximately square beam of 100 μm x 100 μm at the sample surface. The sample was oriented with the silicon substrate facing the incoming beam to reduce the possibility of beam damage, where the transmission through a 300 mm diameter silicon wafer is ≈ 45%. Diffracted intensity was recorded on a 2-D charge coupled device (CCD) detector with square pixels of side length (78.75 ± 0.05) μm. The sample-detector distance was set to (739.0 ± 0.1) cm. The direct beam was blocked by a circular beamstop to prevent detector damage. Fig. 2 (right) is a representative CD-SAXS diffraction pattern. Intensities were recorded as a function of the scattering vector, q (= $4\pi/\lambda \sin(\theta)$, where 2θ is the angle of diffraction), and x denotes an axis parallel to the main axis of

diffraction. The beam origin (i.e., q = 0) is defined at the beam center on the detector. X-rays diffracted from the test pattern are symmetrically diffracted about the beam center, making I(q) = I(-q). As a result, the intensities presented here are an average of I(q) and I(-q), hereafter labeled simply as q. The Fourier space plane, $q_x - q_y$, is closely approximated by the detector plane with the q_x axis oriented along the main axis of diffraction. The data reported here are taken with the beam at normal incidence to the substrate plane.

Due to a lack of phase information in the scattered intensity measured by CD-SAXS, the data must be modeled assuming an average cross-sectional shape of the line/space pattern. Fig. 3 is a 3-D model for the line profiles where *w* is the bottom CD, *H* is the line height and α is the sidewall angle. In this model, the sidewall angle is kept constant while the sidewall modulates along the line direction with amplitude (*A*). A simultaneous weighted nonlinear least square fitting of the diffraction intensity on the equator (I_0) and on the satellite (I_1) could give the average CD ($w_{ave} = w - H \tan\alpha$), the programmed roughness amplitude (*A*), and the total line edge roughness (σ). A weighted nonlinear least square 2-D fitting of the q_x-q_z intensity map will deconvolute the bottom CD and sidewall angle. A detailed data analysis approach is available elsewhere.[7]

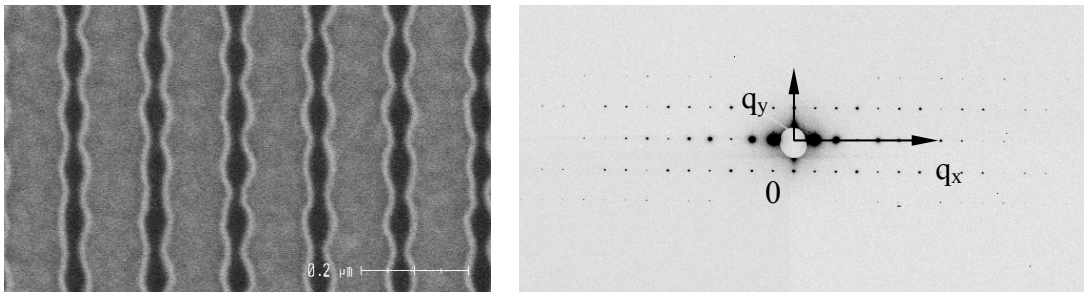

Fig. 2. A top down CD-SEM image displays the magnitude and periodicity of the programmed roughness in the photoresist line/space pattern (left). CD-SAXS two-dimensional detector image of a sample with programmed periodic line width roughness (right). The scattering vectors along the diffraction axis (q_x) and normal to the diffraction axis (q_y) are shown. In addition to the main diffraction axis at q_y = 0 nm-1, a series of satellite diffraction peaks are found at $q_y = \pm 2\pi/\lambda$, where λ is the wavelength of the tab spacing.

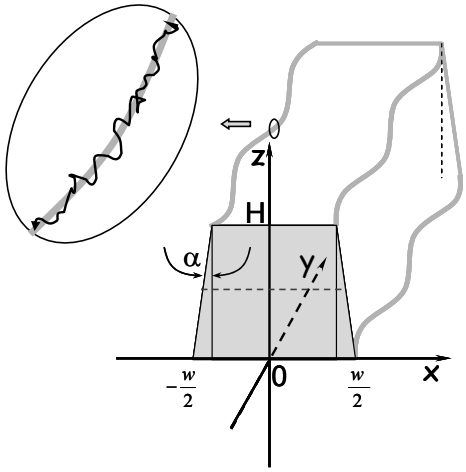

Fig. 3. A 3-D model used for CD-SAXS data analysis where *w* is the bottom line width, α is the sidewall angle, and *H* is the line height. The cross section was modeled as a symmetrical trapezoidal shape while the sidewall edge shifts with a sine function along the line. The magnified part of the line edge in the figure schematically shows the naturally random roughness that is coupled with the programmed modulation.

3. RESULTS AND DISCUSSION

Fig. 2 (right) displays a typical diffraction pattern obtained from line/space patterns with periodic LWR. In addition to the main diffraction axis observed along $q_y = 0$, two parallel, or "satellite," axes of diffraction are observed symmetrically above and below the main axis. The parallel diffraction axes are characteristic of a programmed line edge roughness with a single period L that travels along the line direction. The satellite peak diffraction arises from the constructive interference of the periodically placed tabs on the line edges. The intensity is therefore directly relatable to the volume of LWR. We extract a quantitative measure of the amplitude of periodic LWR by performing weighted nonlinear least square fits of the intensity profile of the main diffraction axis and satellite peaks simultaneously.[5] The results of the programmed line edge roughness (amplitude) and non-programmed line edge roughness dependence on focus positions are shown in Fig. 4.

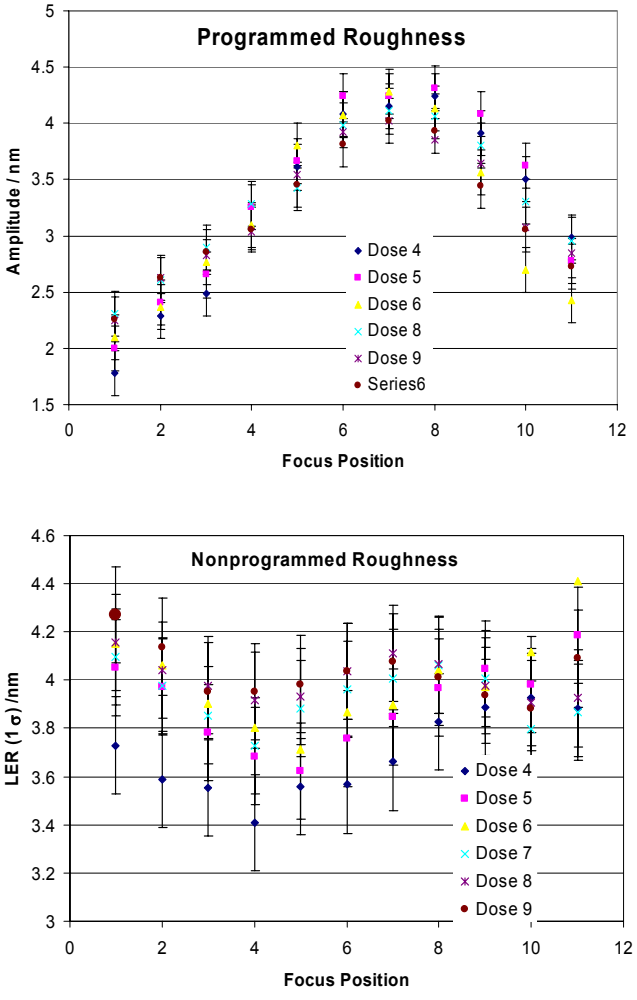

Fig. 4. a.) The amplitude of programmed LER dependence on focus and dose (left). b.) The non-programmed LER dependence on focus and dose (right). The LER parameter includes contributions from the natural line edge roughness, sidewall angle, height variation, and other irregular variations in line width. They were decoupled by a simultaneous weighted nonlinear least square fitting of the diffraction intensity profile on the main diffraction axis and the satellite peaks.

Fig. 4 clearly shows that the focus positions have opposite effects on the programmed and non-programmed line edge roughness. The programmed LER is a tiny feature that was fabricated intentionally while the non-programmed LER represents the traditional LER fluctuations associated with the fabrication process. Consequently, the larger value

for the programmed line edge roughness indicates higher fidelity transfer from the hardmask; however, the larger value for non-programmed line edge roughness shows that a substantial loss in resolution occurs during pattern transfer into the nitride layer. The amplitude of the programmed line edge roughness could be used as a measure of the fidelity of feature transfer in the lithography process. The programmed and non-programmed LER together can serve as a gauge to optimize the focus parameter, similar to the well known Bossung curves in the lithography process. In this work, the optimized focus occurred at a focus position between 6 and 8 where the amplitude of programmed line edge roughness is maximum and of non-programmed line edge roughness is minimum.

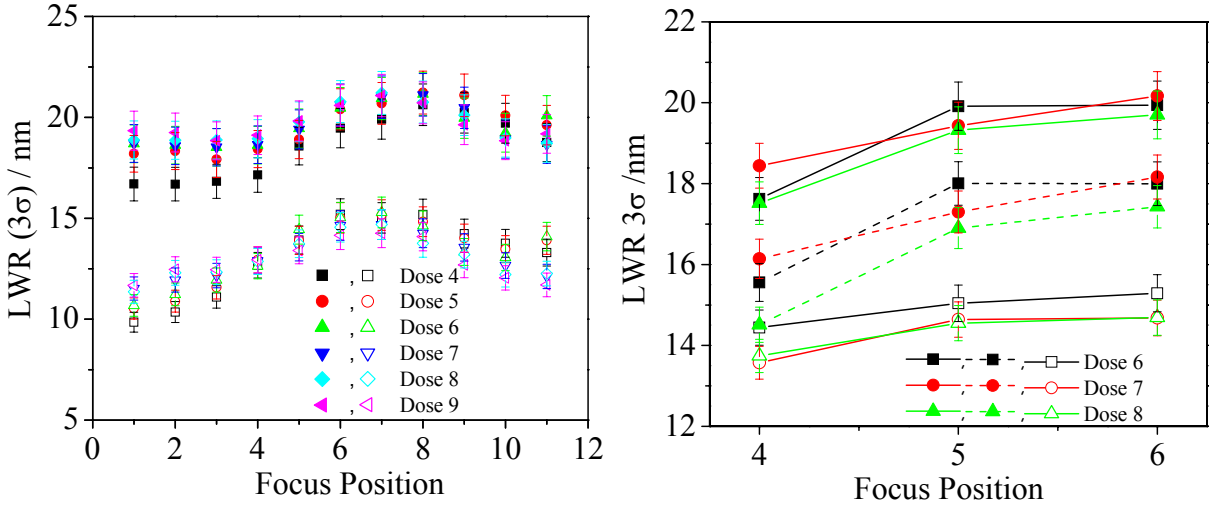

Fig. 5. a.) Total LWR measured by CD-SAXS (solid) and CD-SEM (open) dependence on focus position and exposure dose (left). b.) LWR with natural roughness but without the sidewall angle component contribution by CD-SAXS (solid symbol + line), sole programmed LWR by CD-SAXS (solid symbol + dash line) and LWR by CD-SEM (open) dependence on focus position and exposure dose. Presented data coveredonly a 3 x 3 sub-matrix of focus and dose.

To compare the results by CD-SEM measurements, we converted the programmed line edge roughness and non-programmed line edge roughness into one total line width roughness shown as Fig. 5(a). Unlike Fig. 4, the LWR cannot be used as a gauge to optimize the focus effect. Overall, Figure 5(a) shows that the LWR determined by CD-SAXS tracks very well with that determined by CD-SEM for the entire focus-dose matrix. However, the LWR obtained from CD-SEM is always ≈ 8 nm smaller than the value obtained from CD-SAXS. To clarify the difference between two methods, the sidewall angle component contribution was decoupled from the CD-SAXS LWR number as shown in Fig. 5 (b). It clearly shows that the LWR that includes natural roughness but no sidewall angle is about 2 nm larger than the LWR from sole programmed line roughness. As expected, differences in the LWR values as measured by CD-SAXS and CD-SEM narrows down to ≈ 5 nm. But unexpectedly, the LWR from sole programmed line edge roughness is still about (2 to 3) nm larger than CD-SEM measurements. One possible reason is that CD-SEM measurements underestimate the LWR because the line edge profile in SEM is defined by selection algorithms for threshold. This image analysis process may smooth out some high frequency random roughness fluctuations that are measured by CD-SAXS. Another possible source of this discrepancy could be a difference in sensitivity between the CD-SEM and CD-SAXS to different periodicities of roughness, i.e., different bandwidth windows of the roughness power spectrum. Each CD-SEM image includes a 2 μm long segment of line, whereas the CD-SAXS spot is larger and thus may include some components of longer wavelength roughness. Further investigations are ongoing to clarify these differences between the CD-SAXS and CD-SEM measurements.

Fig. 6a compares a Mandel plot[12] of the average CD measured by CD-SAXS with CD measured by CD-SEM using total measurement uncertainties (TMU). The correlation coefficient (slope) is (0.94 ± 0.06). However, there is an offset of (-13.03 ± 0.37) nm. The offset is a result of differences that arise from the different physical principles that govern each measurement method. In CD-SEM measurements, the image analysis algorithms weight the bottom CD while the a normal incident X-ray scattering always gives an average CD as illustrated in Fig. 2. When the cross-sectional profile is trapezoid, the average CD is always smaller than the bottom CD. A further verification was shown in Fig 6b. where the

bottom CD was measured by rotational CD-SAXS. The Mandel plot of the bottom CD in Fig 6 correlates well with the comparison of CD-SAXS and CD-SEM measurements. TMU analysis gives a correlation coefficient (0.92 ± 0.07) and average offset (-3.5 ± 2) nm. The offset was largely reduced to near zero compared with the normal incidence measurements. The coincidence of average CD and bottom from CD-SAXS also confirms that the cross-sectional profile is approximately trapezoidal shape. This comparison also confirms that both CD-SEM and CD-SAXS can work well for large gratings. For samples with smaller pitches, the comparison work is undergoing. In principle, CD-SAXS can measure smaller features more precisely. With these capabilities, one promising initial application of CD-SAXS is to serve as a high precision reference measurement method for CD-SEM calibration for sub-32 nm manufacturing and beyond.

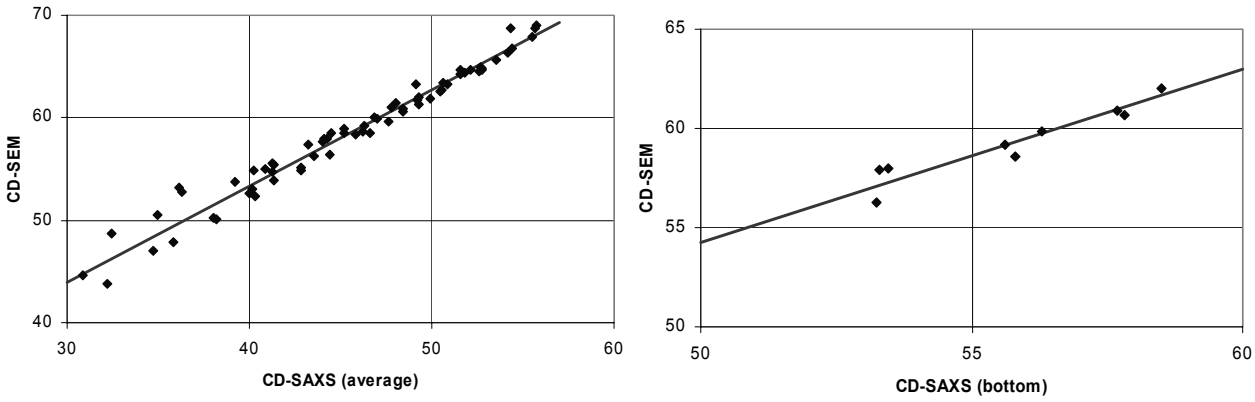

Fig. 6 a) The Mandel plot of bottom CD by normal incidence CD-SAXS versus CD-SEM measurements. A TMU analysis gives a slope (0.94 ± 0.06) and an offset (-13.03 ± 0.37) nm. b) The Mandel plot of bottom CD by rotational CD-SAXS versus CD-SEM measurements. A TMU analysis gives a slope (0.92 ± 0.07) and average offset (-3.5 ± 2) nm. In two plots, the unit is nanometers. The square dots are the input data and the line is the TMU fitting.

Fig. 7 shows an example of CD-SAXS measurement repeatability with 50 repeat runs for 10 s and 20 s. The CD has a standard error of 0.1 nm within 90% confidence that the precision value is within 10% of the value listed, based on the sampling plan, with minimal trend to the data (non-destruction of the data). LWR has a standard error of 0.4 nm and 0.3 nm for 10-s and 20-s measurements. The 20-s measurement had a higher signal-to-noise ratio.

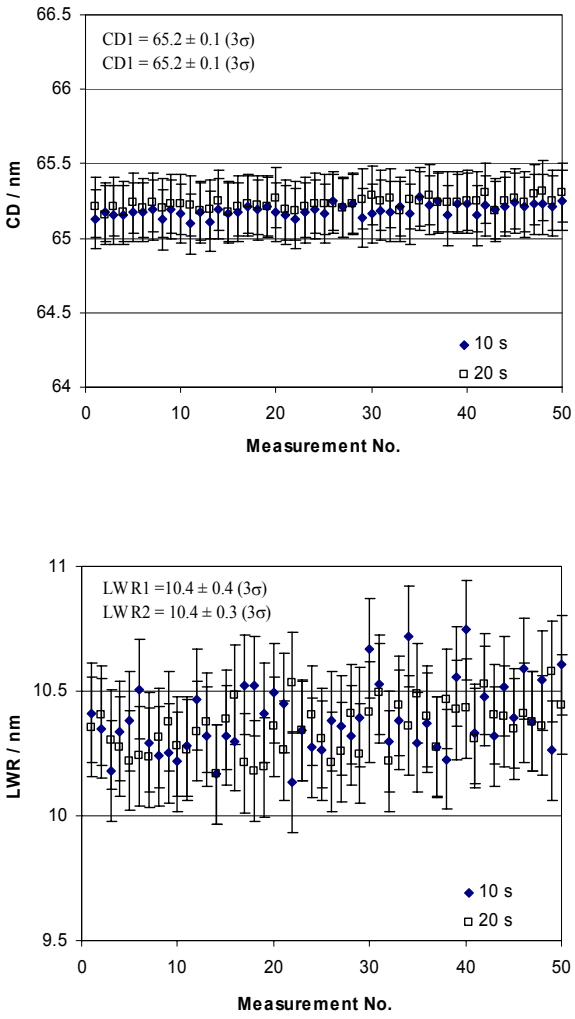

Fig. 7 Static repeatability measurement (50 times) for small angle X-ray data collection time for 10 s and 20 s per measurement (based on sample plan with minimal trend to the date) (a) CD, 3σ precision is 0.1nm, (b) LWR: 3σ precision is 0.4 nm and 0.3 nm for 10-s and 20-s measurements, respectively.

4. CONCLUSIONS

In this report, the capabilities of critical dimension small angle X-ray scattering (CD-SAXS) were evaluated and compared to analogous results from critical dimension scanning electron microscopy (CD-SEM). CD-SAXS can decouple the programmed and non-programmed line edge roughness. These results show that CD-SAXS measurements can be used to optimize the focus parameter in the lithography process on well behaved samples with a known profile and with a predicatable height. The preliminary results were very encouraging, suggesting this technology could be advanced to serve as an online monitor tool.

5. ACKNOWLEDGEMENTS

This work was supported by Intel under CRADA 1893 and the NIST Office of Microelectronics Programs. The authors acknowledge George Thompson and Melissa Shell at Intel Corporation for their support, the ISMI/SEMATECH Advanced Litho Metrology Advisory Group (AMAG), and the Metrology Program Advisory Group (MPAG) for their continuing support. Support for CD-SAXS experiments was provided by Steven J. Weigand and Denis T. Keane at the 5-DND-ID beamline (DND-CAT) at the Advanced Photon Source. Use of the Advanced Photon Source was supported by the U. S. Department of Energy, Office of Science, Office of Basic Energy Sciences, under Contract No. DE-AC02-06CH11357.

6. REFERENCES

1. R. L. Jones, T. Hu, E. K. Lin, W.-L. Wu, R. Kolb, D. M. Casa, P. J. Bolton, G. G. Barclay, Appl. Phys. Lett. **83**, 4059 (2003).
2. T. Hu, R. L. Jones, W.-L. Wu, E. K. Lin, Q. Lin, D. Keane, S. Weigand, J. P. Quintana, J. Appl. Phys. **96**, 83 (2004).
3. R. L. Jones, T. Hu, C. L. Soles, E. K. Lin, W.-L. Wu, D. M. Casa, A. Mahorowala, Proc. SPIE **5375**, 191 (2004).
4. R. L. Jones, W.-L. Wu, C-Q Wang, E. K. Lin, K.-W Choi, B. J. Rice, G. M. Thompson, S. J. Weigand, D. T. Keane, Proc. SPIE **6152**, 61520N (2006).
5. C. Wang, R. L. Jones, E. K. Lin, W.-L. Wu and J. Leu, Appl. Phys. Lett., **90**, 193122 *(2007)*.
6. C. Wang, R. L. Jones, E. K. Lin, W.-L. Wu, B. J. Rice, K.-W. Choi, G. Thompson, S. J. Weigand, and D. T. Keane, J. Appl. Phys. **102**, 024901 (2007).
7. C. Wang, R. L. Jones, E. K. Lin, W.-l Wu, J. S. Villarrubia, K.-W. Choi, J. S. Clarke, B. J. Rice, M. J. Leeson, J. Roberts, R. Bristol, B. D. Bunday, Proc. SPIE 6518, 6518O, (2007)
8. C. Wang, R. L. Jones, K.-W. Choi, D. L. Ho, C. Soles, E. K. Lin, W.-L. Wu, J. S. Clarke, J. S. Villarrubia, B. Bunday, "CD-SAXS Measurements Using Laboratory Based and Synchrotron Based Instruments," Proc. SPIE, 6922, 6922-85 (2008).
9. B. Bunday, D. McCormack, M. Bishop, J. Villarrubia, A. Vladar, R. Dixson, T. Vorburger, N. Orji and J. Allgair, Proc. SPIE XVIII, 515 (2004).
10. D.L. Ho, C. Wang, E. K. Lin, R. L. Jose and W.-L. Wu, AIP Conference Proceedings, 931, 382, 2007.
11. SEMI P47-0307 Test Method for Evaluation of Line-Edge Roughness and Linewidth Roughness. March 2007.
12. Benjamin Bunday, John Allgair, Bill Banke, Chas Archie, Eric Solecky, Amir Azordegan, Kye-Weon Kim and Richard Silver. *Unified Advanced Optical Critical Dimension (OCD) Scatterometry Specification for sub-65 nm Technology* (2007 version), ISMI document # 04114596D-ENG. non-confidential document, available for download at www.sematech.org.
13. The data in this letter, in the figures, and in the tables are presented along with the standard uncertainty (±) involved in the measurement, where the uncertainty represents one standard deviation from the mean.